Draft version September 14, 2015
Preprint typeset using LaTeX style emulateapj v. 04/17/13



# BEYOND THE MAIN SEQUENCE: TESTING THE ACCURACY OF STELLAR MASSES PREDICTED BY THE PARSEC EVOLUTIONARY TRACKS

Luan Ghezzi[1] & John Asher Johnson[1]

*Draft version September 14, 2015*

## ABSTRACT

Characterizing the physical properties of exoplanets, and understanding their formation and orbital evolution requires precise and accurate knowledge of their host stars. Accurately measuring stellar masses is particularly important because they likely influence planet occurrence and the architectures of planetary systems. Single main-sequence stars typically have masses estimated from evolutionary tracks, which generally provide accurate results due to their extensive empirical calibration. However, the validity of this method for subgiants and giants has been called into question by recent studies, with suggestions that the masses of these evolved stars could have been overestimated. We investigate these concerns using a sample of 59 benchmark evolved stars with model-independent masses (from binary systems or asteroseismology) obtained from the literature. We find very good agreement between these benchmark masses and the ones estimated using evolutionary tracks. The average fractional difference in the mass interval $\sim$0.7 – 4.5 $M_{\odot}$ is consistent with zero (-1.30 $\pm$ 2.42%), with no significant trends in the residuals relative to the input parameters. A good agreement between model-dependent and -independent radii (-4.81 $\pm$ 1.32%) and surface gravities (0.71 $\pm$ 0.51%) is also found. The consistency between independently determined ages for members of binary systems adds further support for the accuracy of the method employed to derive the stellar masses. Taken together, our results indicate that determination of masses of evolved stars using grids of evolutionary tracks is not significantly affected by systematic errors, and is thus valid for estimating the masses of isolated stars beyond the main sequence.

*Keywords:* stars: fundamental parameters — stars: evolution — binaries: general — asteroseismology

## 1. INTRODUCTION

A complete understanding of the formation and evolution of planetary systems requires a detailed knowledge of the physical properties of the planets and their host stars. A subject of intense study within exoplanetary science are the nature of the links between planets and the stars they orbit. Planets form from the same molecular cloud material from which their host stars form, so planets can be thought of as the leftover relics of the star-formation epoch. Similarly, stars can be studied as relics of the environment from which planets formed long ago (Laughlin et al. 2004; Fischer & Valenti 2005; Kennedy & Kenyon 2008; Johnson 2008). Relationships between planetary systems observed today and their host star's physical properties therefore provide important constraints on theories of planet formation and orbital evolution.

The two key physical properties that govern stellar evolution are mass and chemical composition, and these characteristics of host stars are thought to be linked to the formation and orbital evolution that produced the architectures of planetary systems seen today. Many independent studies have shown that the occurrence of giant planets around FGK dwarfs and post-main-sequence stars such as subgiants strongly increases with the stellar iron abundance (e.g., Gonzalez 1997; Santos et al. 2004; Fischer & Valenti 2005; Johnson et al. 2010a). However, there exists much debate as to whether this correlation between metallicity and giant planet occurrence exists for stars on the red giant branch (e.g, Johnson et al. 2010a; Maldonado et al. 2013; Mortier et al. 2013; Jofré et al. 2014; Reffert et al. 2015) or stars that host planets with masses less than that of Neptune (e.g., Ghezzi et al. 2010b; Sousa et al. 2011; Buchhave et al. 2014). Evidence for possible connections between the presence of planets and other peculiarities in the chemical abundances of their stellar hosts are still ambiguous (see, e.g., Adibekyan et al. 2012, 2014; Figueira et al. 2014; Teske et al. 2014; and references therein).

Also still unclear is the role of stellar mass on the formation and evolution of extrasolar planets. Planet-search programs based on the radial velocities (RVs) technique have mainly targeted Solar-type stars because they are relatively numerous and bright in the Solar neighborhood, and their spectra have a considerable number of unblended, narrow metallic lines, allowing more precise measurements of both the Doppler shifts and stellar properties (e.g. Galland et al. 2005; Lagrange et al. 2009; Becker et al. 2015). One direct consequence of this selection criterion is a relatively small range of stellar masses included among the targets of the largest existing planet-search programs ($\sim$0.7 –1.4 $M_{\odot}$). The extension of this interval to lower-mass M dwarfs was a natural extension of the exoplanet searches (e.g., Johnson et al. 2007a; Bonfils et al. 2013), given these stars are more numerous in the Galaxy and allow robust detections of Earth-like planets with the current instrumental capabilities (e.g., Mayor et al. 2014; Quintana et al. 2014). Nevertheless, the monitoring and characterization of M dwarfs has been challenging because they are faint and their optical spectra are com-

[1] Harvard-Smithsonian Center for Astrophysics, 60 Garden Street, Cambridge, MA 02138 USA; lghezzi@cfa.harvard.edu

pletely dominated by molecular bands (e.g. Bean et al. 2006; Maness et al. 2007). Dedicated ongoing and future surveys will progressively overcome these issues (e.g., Berta et al. 2013; Quirrenbach et al. 2014).

A completely different difficulty is encountered for planet searches around massive stars on the main sequence ($\gtrsim$1.5 $M_{\odot}$). The hotter effective temperatures and higher rotational velocities of early F and A stars produce a spectrum with fewer and much broader lines, hindering the measurement of precise radial velocities and the reliable detection of extrasolar planets (Galland et al. 2005; Becker et al. 2015). However, as these massive stars evolve off the main sequence towards the red giant branch (RGB), they cool and slow down (do Nascimento et al. 2000). As a result, their spectra then show many narrow lines which allow the measurement of Doppler shifts caused by extrasolar planets. Therefore, analyzing the evolved counterparts of main-sequence F- and A-type dwarfs is currently the best alternative to investigate planet occurrence around more massive stars[2].

To this end, more than 1000 evolved stars have been monitored by several surveys (see Niedzielski et al. 2015 and references therein), resulting in the detection of more than 100 planets around them (Jofré et al. 2014). Although this sample is relatively small when compared to the entire sample of discovered planets, some interesting properties already started to emerge, such as a paucity of planets at short orbital distances and large eccentricities (Sato et al. 2007; Bowler et al. 2010; Jones et al. 2014) and the possible lack of a giant planet – metallicity correlation (Ghezzi et al. 2010a; Maldonado et al. 2013; Jofré et al. 2014; but see also Reffert et al. 2015).

Of particular interest to this work is the higher occurrence rate of Jovian planets around more massive stars measured by Johnson et al. (2010a). The analysis of 1194 stars with masses in the range 0.2 – 2.0 $M_{\odot}$ not only provided additional confirmation to the well-established giant planet-metallicity correlation, but also revealed that the occurrence rate of these planets increases linearly from ∼3% for M dwarfs to ∼14% for A stars. This is a very important result because it adds new constraints to the planet formation theories and also provides guidance to ongoing and future surveys monitoring evolved stars (radial velocities and transits) or A dwarfs (direct imaging – Crepp & Johnson 2011).

The determination of masses for these isolated evolved stars relied on the comparison of observed properties with stellar evolutionary tracks (Johnson et al. 2010a, 2011, 2013). The different models usually adopted in this method were subjected to numerous improvements and validation tests over the last few decades, leading to more precise predictions of the stellar parameters and also a better understanding of the processes involved in the evolution of stars (e.g., Vandenberg 1985; Andersen et al. 1988; Andersen 1991; Andersen et al. 1991; Pols et al. 1997; Demarque et al. 2004; Torres et al. 2010; Bressan et al. 2012; Brogaard et al. 2012; Garcia et al. 2014; Torres et al. 2015). For field stars on the main sequence, this technique for determining masses generally provides accurate results (e.g., Torres et al. 2010) that are also fairly consistent with other independent estimates (Pinheiro et al. 2014; but note the possible issues with spectroscopic masses for stars with M $\gtrsim$ 1.2 $M_{\odot}$).

The reliability of the application of this method to subgiants and giants is, however, more uncertain. Although stellar evolution models were able to successfully describe some binary systems with at least one evolved component (e.g., Andersen et al. 1988, 1991; Torres et al. 2015), there were suggestions that the masses of planet-hosting subgiants and giants could have been overestimated (by up to 50%) due to systematic errors on their atmospheric parameters or the models themselves (Lloyd 2011, 2013; Schlaufman & Winn 2013). Additional evidence of possibly overestimated masses for evolved stars with planets (by up to 100%) were recently presented by Sousa et al. (2015) (but note that a possible explanation for some of the problematic stars is given in Section 4.2 of Takeda & Tajitsu 2015). In spite of the growing number of evolved stars with precisely determined masses (through orbital solutions in binary systems or asteroseismology of field or cluster stars), the evolutionary tracks continue to be main method to determine this fundamental parameter for single subgiants and giants. Thus, possible errors in the results would have implications on many different studies, ranging from the formation and architectures of planetary systems to Galactic chemical and dynamical evolution, and have to be carefully investigated.

We and others have been conducting a study to precisely constrain the masses of evolved stars using different input parameters and techniques. The first results of this effort for the bright nearby subgiant star HD 185351 were presented by Johnson et al. (2014). In this work, we check the accuracy of the evolutionary tracks method using a sample of benchmark subgiants and giants with accurate masses. This sample and the literature masses for their masses are described in Section 2, while the determination of corresponding stellar masses from evolutionary tracks is discussed in Section 3. In Section 4, we compare the two sets of masses and show that the evolutionary tracks method do not seem to have any systematic errors that would overestimate the masses of evolved stars. Finally, our concluding remarks are presented in Section 5.

## 2. SAMPLE OF BENCHMARK STARS

Our sample of benchmark stars consists of 59 subgiants and giants with precise masses determined with methods that are based on minimal assumptions and physical modeling. In this study, we focus on dynamical masses measured for stars in binary systems and asteroseismic masses calculated with scaling relations and the *direct method* (i.e., without the usage of [Fe/H] and grids of models to further constrain the evolutionary parameters; see, e.g., Gai et al. 2011).

### 2.1. *Stars in Binary Systems*

We performed an extensive literature search for detached binary systems in which at least one of the components is an evolved star. Most of them were found with

[2] Direct imaging is a promising technique to detect giant planets around B-A stars, but so far only a handful of them were found (see, e.g., Crepp & Johnson 2011; Nielsen et al. 2013 and references therein)

the help of DEBCat[3] (Southworth 2014). Only subgiants and giants that have available values for effective temperature ($T_{\rm eff}$), metallicity ([Fe/H]), $V$ magnitude and parallax ($\pi$) or distance ($d$) were selected. These are the input parameters necessary to obtain masses with the evolutionary track method (see Section 3). We removed any stars with metallicities determined through the best fit to evolutionary tracks or isochrones (e.g., Sandberg Lacy et al. 2012; Ratajczak et al. 2013) in order to avoid dual dependencies on the model tracks, e.g. using [Fe/H] derived from one evolution model grid to interpolate onto another model grid.

Our selection criteria resulted in a sample of 26 evolved stars in 16 binary systems in the Milky Way (MW), Small Magellanic Cloud (SMC) and Large Magellanic Cloud (LMC). These stars are shown in Tables 1 and 2 along with their fundamental parameters, respective uncertainties and literature references. In some cases, no uncertainty was available for the $V$ magnitudes and we adopted $\sigma(V) = 0.01$ for MW stars because this is the typical accuracy of the *Hipparcos* measurements Perryman et al. (1997). For LMC stars, we adopted a conservative uncertainty $\sigma(V) = 0.02$ because the accuracy of photometric calibrations in the OGLE project is better than 0.02 mag (Udalski et al. 2008). We also assumed $E(B-V) = 0.000$ for all stars closer than ∼60 pc. Their positions in a HR diagram can be seen in Figure 1. Dynamical stellar masses and radii were directly determined in the original source papers with precisions of $\lesssim$3% and $\lesssim$7%, respectively, through the analysis of radial velocities (RVs) and light curves. The masses range from ∼1.2 to ∼4.5 $M_{\odot}$.

### 2.2. *Stars with Asteroseismic Parameters*

We conducted a separate literature search for evolved single stars with measurements of the two global asteroseismic parameters: the frequency of maximum power $\nu_{\rm max}$ and the large frequency separation $\Delta\nu$. Once again, we kept only those stars which also had reported, evolution-model-independent values for $T_{\rm eff}$, [Fe/H], $V$ magnitude and parallax ($\pi$) or distance ($d$) (see Section 2.1). The last requirement, in particular, dramatically reduces the number of stars suitable for our study.

We calculated asteroseismic masses and radii with the *direct method*, using published values of $\nu_{\rm max}$, $\Delta\nu$ and $T_{\rm eff}$ as input to the scaling relations (e.g., Kjeldsen & Bedding 1995) written as:

$$\frac{M}{M_{\odot}} \simeq \left(\frac{\nu_{\rm max}}{\nu_{\rm max,\odot}}\right)^{3} \left(\frac{\Delta\nu}{\Delta\nu_{\odot}}\right)^{-4} \left(\frac{T_{\rm eff}}{T_{\rm eff,\odot}}\right)^{3/2} \quad (1)$$

$$\frac{R}{R_{\odot}} \simeq \left(\frac{\nu_{\rm max}}{\nu_{\rm max,\odot}}\right) \left(\frac{\Delta\nu}{\Delta\nu_{\odot}}\right)^{-2} \left(\frac{T_{\rm eff}}{T_{\rm eff,\odot}}\right)^{1/2}. \quad (2)$$

The reference solar asteroseismic parameters $\nu_{\rm max,\odot} = 3090 \pm 30$ $\mu$Hz and $\Delta\nu_{\odot} = 135.1 \pm 0.1$ $\mu$Hz (Huber et al. 2011) were adopted in the above equations, as well as the canonical value $T_{\rm eff,\odot} = 5777$ K. We note that, while these results are independent from stellar evolution models, they do rely on scaling of solar p-modes to stars of different masses, metallicities and evolutionary states. Recent studies have shown that the usage of the scaling relations for metal-poor or evolved stars require some caution (e.g., Miglio et al. 2012; Epstein et al. 2014). However, many different tests indicate that these scaling relations provide masses and radii with accuracies ∼10% and ∼5%, respectively (see discussion in Section 2.4.1 of Johnson et al. 2014). No corrections were applied to the scaling relations because there is still no consensus which of the proposed ones works best (e.g., Brogaard et al. 2014). Nevertheless, the shifts in $M$ and $R$ that would be caused by adopting the available corrections are discussed in Section 4.

We should also note that Equations 1 and 2 contain the stellar effective temperature, which in turn can

[3] http://www.astro.keele.ac.uk/jkt/debcat/

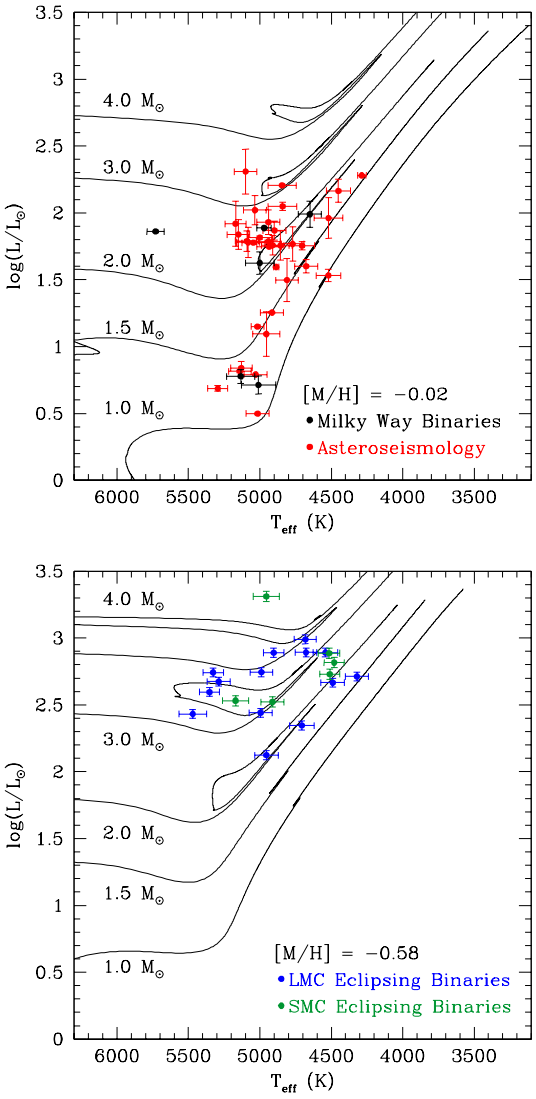


**Figure 1.** HR diagrams showing the positions of stars in our sample. The upper panel shows the MW binaries (black points) and field stars with asteroseismology (red points). The lower panel presents the eclipsing binaries (EBs) from LMC (blue points) and SMC (green points). In all panels, the solid lines represent PARSEC evolutionary tracks (Bressan et al. 2012) for 1.0 $M_{\odot}$, 1.5 $M_{\odot}$, 2.0 $M_{\odot}$, 3.0 $M_{\odot}$ and 4.0 $M_{\odot}$, and representative metallicities for the depicted samples.

be determined using model-dependent techniques (for instance, spectroscopic $T_{\rm eff}$ depends on model atmospheres). However, we note that the dependence of the stellar radius on $T_{\rm eff}$ in Equation 2 is weak relative to the other terms. Moreover, the uncertainties on the values of masses and radii caused by typical errors on the effective temperatures ($\sim$80 K or $\sim$2% considering a typical $T_{\rm eff}$= $\sim$4900 K) are negligible (of order 1%).

As one of our goals is to define a statistically significant sample of benchmark stars, we decided to remove stars for which the uncertainties in the asteroseismic masses were higher than 20%. After this cut, we obtained a subsample of 33 evolved stars with asteroseismic parameters and masses with typical precisions ranging from 5% to 20%. These relatively large errors could be decreased if we used a grid-based asteroseismic method (Gai et al. 2011), in which the stellar properties predicted by a grid of stellar evolution models are converted to the asteroseismic parameters $\nu_{\rm max}$ and $\Delta\nu$, and then compared to the observed values. But the goal of this work is to avoid any model dependencies in the reference parameters of the benchmark stars sample.

Our asteroseismic benchmark stars are shown in Tables 1 and 2. As for the binaries, $\sigma(V) = 0.01$ was adopted for stars with no uncertainties available for $V$. We assumed $E(B-V) = 0.000$ for all stars closer than $\sim$60 pc as well as 10 eight more distant stars for which no values were available in the literature. When no uncertainties were not reported for the asteroseismic parameters, arbitrary errors of 5% and 2% were adopted for $\nu_{\rm max}$ and $\Delta\nu$, respectively (following Bruntt et al. 2010). The positions of the stars in a HR diagram is shown in Figure 1 and their masses range from roughly 0.7 $M_{\odot}$ to 4.0 $M_{\odot}$. One star (KIC 8410637) is common to both the binary and asteroseismic samples. In this case, we adopt the more precise dynamical stellar mass and radius[4].

### 2.3. *Final Sample*

Our final sample consists of 59 benchmark stars with precise dynamical or asteroseismic masses. According to model-dependent classifications provided in the reference papers or to Figure 1, we can see that most of our stars are on the red giant branch (RGB) or on the red clump (RC), which are also the regions on the H–R diagram targeted by many planet-search surveys that focus on evolved stars (e.g., Hatzes et al. 2005; Sato et al. 2005; Lovis & Mayor 2007; Lee et al. 2011; Omiya et al. 2012; Niedzielski et al. 2015; Reffert et al. 2015). All of them have the required parameters to allow an independent determination of their masses using stellar evolution models (see section 3).

As explained in the previous sections, some stars were removed from our sample because they did not fulfill one or more of our selection criteria. For completeness, those stars are listed in Table 3 along with the selected references and the reasons for their exclusion. It is also worth noting that we may have overlooked a few stars despite our best efforts to conduct a thorough literature search[5]. However, we consider that our current sample is statistically robust, and the addition of a few objects will not likely affect our conclusions.

## 3. STELLAR MASSES FROM EVOLUTIONARY TRACKS

We derived model-dependent stellar masses for all 59 of our benchmark stars using stellar evolution model tracks. In this method, measured stellar properties (typically, $T_{\rm eff}$, log–luminosity $\log_{10}(L/L_{\odot})$, and metallicity [Fe/H]) are compared with the properties predicted by evolution models calculated for different initial masses and chemical compositions (e.g. Girardi et al. 2002; Dotter et al. 2008; Demarque et al. 2008). A probabilistic analysis then provides the best match between the observed and theoretical properties of the star, allowing the determination of its mass (as well as radius and age). This method is known to work well for solar-type stars on the main sequence (e.g., Torres et al. 2010), but has not been extensively tested on for stars in advanced evolutionary states (however, see Johnson et al. 2013, 2014). Testing these model grids using a large sample of evolved stars is the primary goal of this study.

We adopted the implementation of the method contained in the PARAM code, which was kindly provided by Leo Girardi[6]. Estimates of the mass, radius, $\log g$ and age are obtained through a Bayesian estimation method using different priors, input parameters and isochrones (da Silva et al. 2006). We adopted the default options for the Bayesian priors and selected the new PARSEC isochrones from Bressan et al. (2012). We also chose the analysis of stars with known parallaxes, for which we provided the additional input parameters $T_{\rm eff}$, [Fe/H] and V magnitude (see Table 1). Extinction corrections $A_V$ were applied to the V magnitudes of all stars farther than 60 pc for which a reddening value $E(B-V)$ was available in the literature. The standard relation $A_V = 3.1E(B-V)$ was adopted for the conversion of reddening to $V$-band extinction.

It is worth noting that the Padova models (in their most recent version, PARSEC; Bressan et al. 2012) were chosen because its wide usage in the literature, including the estimation the properties of evolved stars (e.g., Johnson et al. 2006, 2007b; Döllinger et al. 2007, 2009; de Medeiros et al. 2009; Ghezzi et al. 2010a,b). Tests with other grids of evolutionary tracks are beyond the scope of the present work, but will be adressed in a future contribution using the same sample of benchmark stars.

The masses derived with the evolutionary tracks are shown in Table 2 along with the other output parameters of PARAM and their respective uncertainties. For the giant star $\nu$ Ind, the error on [Fe/H] was arbitrarily increased to 0.20 dex because the PARAM code was not returning valid solutions with the original value ($\sigma_{\rm [Fe/H]} = 0.07$). After some tests, it was clear that PARAM was having issues due to the relatively low metallicity and small original uncertainty. The precision of the masses obtained with the evolutionary tracks method varies from $\sim$2% to $\sim$29%, with a typical (median) value of $\sim$10%. The relative uncertainties on the masses are similar for the samples of binaries and asteroseismic targets and increase for stars with lower effective

[4] The dynamical and asteroseismic masses, radii and surface gravities agree within 1.6$\sigma$ (see Table 2).

[5] Please, contact the authors if you have identified such a case.

[6] For the web interface maintained by Leo Girardi at the Osservatorio Astronomico di Padova, visit http://stev.oapd.inaf.it/cgi-bin/param.

temperatures and larger errors on their metallicities.

## 4. RESULTS AND DISCUSSION

### 4.1. *Masses*

Our comparison between model-independent masses and the corresponding values derived from evolutionary tracks (see Section 3) is shown in Figure 2. We can see there is an overall good agreement and no systematic offsets for the entire mass range ($\sim$0.7 – 4.5 $M_{\odot}$), even though our results are based on a heterogeneous data set. The average absolute and percentage differences between evolutionary track and reference masses for the entire sample and the two subsamples (binaries and asteroseismic targets) are shown in Table 4. We can see that the global average differences are consistent with zero within the uncertainties, with 40 and 33 stars (i.e., 68% and 56% of the sample, respectively) showing agreements between the two mass estimates within 20% and 10%, respectively. The separate results for the binary and asteroseismic samples are somewhat different. While the average mass difference for the former is zero within the errors, it reveals that the evolutionary track results are slightly underestimated for the latter. We therefore see no evidence that the models overpredict the masses of individual stars, in contrast to the concerns raised by Lloyd (2013) and Schlaufman & Winn (2013). Note, however, that the stars analyzed here and in those works are in different evolutionary stages.

We performed weighted linear fits to the fractional residuals of the whole sample as well as the asteroseismic and binary subsamples individually. The weights were calculated as $1/\sigma^2_{total}$, where $\sigma_{total}$ is the fractional uncertainty obtained with the propagation of errors for the difference of the two mass estimates. The results of the fits are listed in Table 4 and demonstrate that a slight trend is observed for the asteroseismic subsample, with the model grids underpredicting stellar masses by an amount that increases with mass. This is also clear from the lower panel in Figure 2.

The results for the asteroseismic targets deserve some further discussion. Thirteen out of 33 stars have fractional differences larger than 20%: Arcturus, $\beta$ Aql, $\delta$ Eri, $\eta$ Ser, HD 170008, HD 170231, HD 178484, KIC 4044238, KIC 6101376, KIC 7909976, KIC 8508931, KIC 8813946, and $\xi$ Hya. Kallinger et al. (2010) derive a mass $M_{\star} = 0.80 \pm 0.20\ M_{\odot}$ for Arcturus (using $\Delta\nu$ and an interferometric radius), which agrees better with the value derived here from the evolutionary tracks ($M_{\star} = 0.98 \pm 0.06\ M_{\odot}$ ). The adoption of the larger asteroseismic mass would reduce the fractional difference from 45% to 22%. Bruntt et al. (2010) provide alternative masses for $\beta$ Aql, $\delta$ Eri and $\eta$ Ser: $M_{\star} = 1.26 \pm 0.18\ M_{\odot}$ (calculated from $\nu_{\rm max}$, $T_{\rm eff}$ and interferometric radius), $M_{\star} = 1.33 \pm 0.07\ M_{\odot}$ (calculated from $\Delta\nu$ and interferometric radius) and $M_{\star} = 1.45 \pm 0.21\ M_{\odot}$ (calculated from $\nu_{\rm max}$, $T_{\rm eff}$ and luminosity), respectively. All these literature masses are in better agreement with the ones obtained from evolutionary tracks and their usage would decrease the fractional differences from 31%, 36% and 30% to 10%, 12% and 15%, respectively.

KIC 8508931, has an alternative determination of the global asteroseismic parameters. Adopting the results from Hekker et al. (2011) (but using the same $T_{\rm eff}$ as before and assuming uncertainties of 5% in $\nu_{\rm max}$ and 2% in $\Delta\nu$), we obtain a mass $M_{\star} = 2.54 \pm 0.43\ M_{\odot}$, which reduces the discrepancy from 26% to 12%. For KIC 8813946, Huber et al. (2012) found a conflict between the radii calculated for this star using different constraints (asteroseismic parameters and angular diameter from interferometry coupled with the parallax) and argue that this discrepancy could be indicative of a problem with the revised *Hipparcos* parallax (van Leeuwen 2007). This problem would, in turn, affect our mass determined from the evolutionary tracks. Finally, the star $\xi$ Hya also has an alternative mass $M_{\star} = 2.89 \pm 0.23\ M_{\odot}$ from Bruntt et al. (2010), calculated from $\nu_{\rm max}$, $T_{\rm eff}$ and its interferometric radius. The adoption of this mass would improve the agreement, with a decrease in the fractional difference from 23% to 16%. Unfortunately, we were not able to find alternative parameters for the stars HD 170008, HD 170231, HD 178484, KIC 4044238, KIC 6101376, and KIC 7909976.

If we replace the masses of the problematic stars with the alternative values mentioned above for six of them, the average differences become: $\langle \Delta M \rangle$ = -0.22 $\pm$ 0.07 $M_{\odot}$ and $\langle \Delta M/M_{Ref.} \rangle$ = -7.18 $\pm$ 2.80%. We can see that the fractional average difference became more negative because the large positive values of Arcturus, $\beta$ Aql and $\delta$ Eri were decreased in the first case and replaced by negative offsets for the other two stars. The absolute average difference did not change significantly and no improvement in the standard deviations of the mean was observed. The parameters of the linear fit, on the other hand, were slightly improved: $A = -7.98 \pm 2.34$, $B = 2.76 \pm 5.07$, $R^2 = 0.274$ and $\sigma = 0.77$. Therefore, it is clear that part of the trend observed for the asteroseismic targets was caused affected by these six stars with large discrepancies and, with the exception of $\eta$ Ser, located at the edges of the mass interval covered by the sample. The remaining trend in the residuals can be mostly attributed to the other seven stars with large deviations and no alternative parameters to be tested.

Corrections to the scaling relations have been proposed by White et al. (2011) and Mosser et al. (2013), but further tests are still necessary to confirm their accuracy. As a test, we applied the latter to the 33 stars in our asteroseismic sample (the former is valid only down to $T_{\rm eff}$ = 4700 K and some stars in the sample are cooler than this limit) and observed a typical decrease in the asteroseismic masses of $\sim$5%, which increases the average fractional difference $\langle \Delta M/M_{Ref.} \rangle$ from -4.29% to 0.47%. Although the agreement is better, we decided to keep our original masses because there is still no consensus in the literature regarding the validity of the proposed corrections to the scaling relations or which one works best (e.g., Brogaard et al. 2014).

The exercise of testing alternative parameters could not be performed for the six binaries that have percentage differences larger than 20%: RT CrB B, OGLE SMC 130.5 4296 A, OGLE LMC-ECL-01866 B, OGLE LMC-ECL-03160 A, OGLE LMC-ECL-09660 B and OGLE LMC ECL15620 A. To the best of our knowledge, there are no alternative reference or input parameters that we could use to check if a better agreement is obtained. Also, we were not able to observe any clear pattern in these stars with larger deviations. They are all from different binary systems and their companions seem to yield

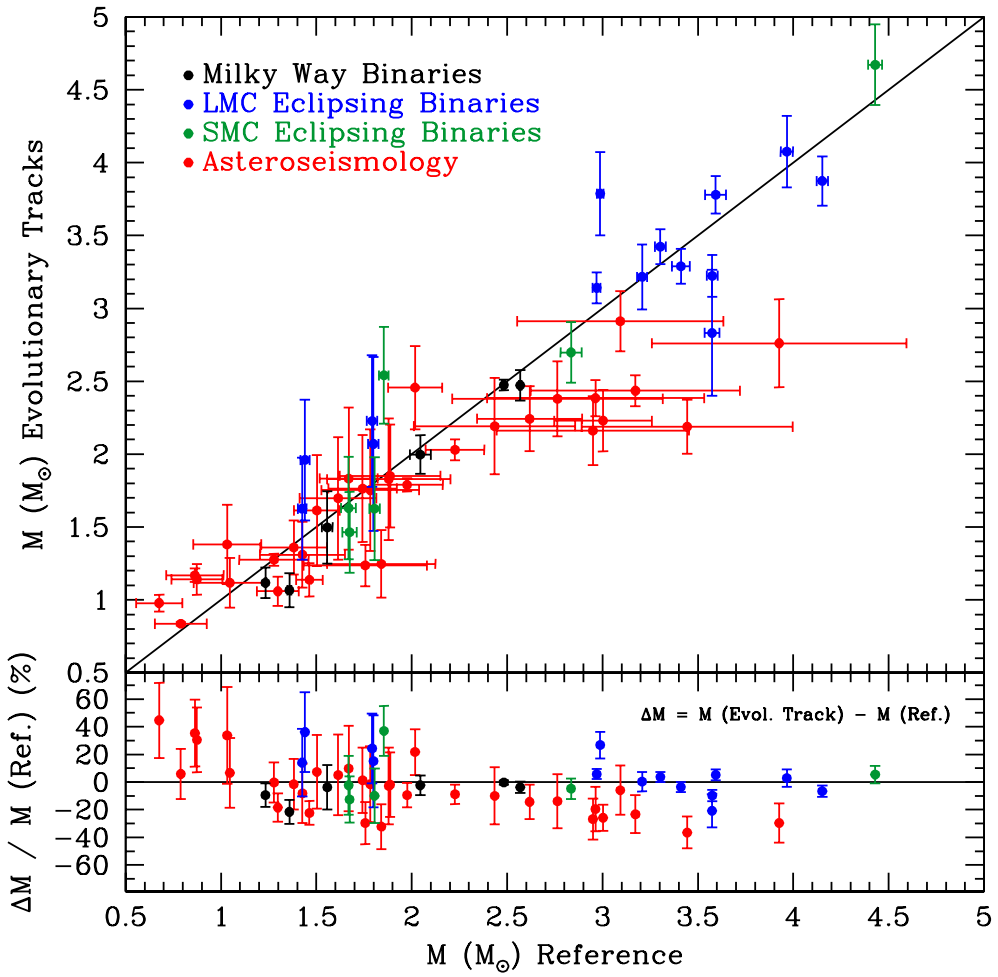


**Figure 2.** Comparison between evolutionary track and reference masses. Milky Way binaries, LMC EBs, SMC EBs and field stars with asteroseismology are shown by black, blue, green and red points, respectively. Black solid lines represent a perfect agreement. The upper panel shows a direct comparison of the masses. The lower panel shows the fractional difference between the mass estimated from the evolutionary tracks and the reference mass. We can see there is a general good agreement between the masses and no significant overestimate of the values by the evolutionary track method.

at least reasonable results (percentage differences lower than 15%). Moreover, they are not all the primary or secondary components in their systems. Thus, it is not feasible to attribute any problems to the analysis or the parameter determination for specific systems. The only detail worth noting is that four of the six stars are from the LMC, i.e., are extragalactic in origin.

We also investigated if the larger fractional differences could be caused by the degeneracy between the two possible evolutionary stages for most stars in our sample: red giant branch (RGB) or the red clump (RC). This degeneracy arises from the identical absolute magnitudes (luminosities) along the ascent of the RGB and stars on the horizontal branch, or red clump region of the H–R diagram. Uncertainties in the effective temperatures and metallicities of these high-luminosity giants therefore results in a double-peaked probability distribution function (PDF) (e.g., da Silva et al. 2006) and this pattern can be indeed observed for many of our stars. A possible consequence of this issue could be the choice of an incorrect mass associated with just one of the peaks (for instance, the mass corresponding to the maximum of the PDF), creating a systematic offset for at least some of the stars in the sample.

Our results do not show such offsets: evolutionary tracks are able to correctly recover the reference masses with an average accuracy better than 10% and no significant systematic trends. This good agreement is related to the way PARAM determines the best solution: it calculates mean values for the parameters from their PDFs, instead of choosing the most likely values, for example. Although this increases the uncertainties on the results, it avoids attributing the parameters to a star given a choice of a specific evolutionary state. Therefore, the possible degeneracies are taken into account in our analysis and do not to seem to be the reason for the most discrepant cases. We should also note that the differences between the two peaks of most of the double-peaked PDFs are within 68.3% confidence interval of the mean value.

As a final check on our results, we checked if the mass differences were a function of any of the parameters that were used as input to the evolutionary tracks method ($T_{\rm eff}$, [Fe/H], $V$ magnitude and parallax). As can be

seen in Figure 3, no systematic trends are found for any of the parameters. The higher correlation coefficients $R^2$ of the weighted linear fits are 0.020 for the entire sample (in $T_{\rm eff}$), 0.014 for the binaries (in [Fe/H]) and 0.124 (in parallax) for the asteroseismic targets.

### 4.2. *Radii*

Our analysis of stellar radii closely follows that of the previous section. The comparison between reference radii and the corresponding values estimated from evolutionary tracks (see Section 3) is depicted in Figure 4. Although the overall agreement is good, we can see a global small offset (∼5%, see Table 4), with the evolutionary tracks underestimating the radii of most stars. There is also a clear difference between the samples of binaries and asteroseismic stars. While the latter have a larger and mostly constant offset with a significant dispersion around it, the former have a smaller dispersion around a small offset that slightly increases with increasing radius. It is worth noting though that these offsets are well within the uncertainties obtained in the radii from evolutionary tracks, as is also clear from Figure 4.

Besides these interesting features, once again we can find asteroseismic targets with percentage differences in radius larger than 20%: $\beta$ Aql, HD 169730, HD 170174, HD 170231, KIC 8508931 and KIC 8813946. Four of them also had problems in their masses. For $\beta$ Aql, our evolutionary track radius (3.25 ± 0.13 $R_\odot$) is in very good agreement with the interferometric value presented by Bruntt et al. (2010) (3.21 ± 0.13 $R_\odot$). Huber et al. (2012) provide an interferometric radius for KIC 8813946 (R = 12.0 ± 1.2 $R_\odot$) which agrees very well with the value derived from the evolutionary tracks (12.0 ± 1.3 $R_\odot$). This could suggest a problem in the asteroseismic global parameters for this star, but we should recall that the parallax is used as an input for both the interferometric and evolutionary track radii. Thus, we can not discard a possible issue on the parallax (as suggested by Huber et al. 2012), which could be leading to two agreeing, but incorrect radii. Finally, adopting for KIC 8508931 the alternative global asteroseismic parameters from Hekker et al. (2011) (but using the same $T_{\rm eff}$ as before and arbitrary uncertainties of 5% in $\nu_{\rm max}$ and 2% in $\Delta\nu$) has a small impact on the radius, reducing the percentage difference from 23% to 19%. Unfortunately, we were not able to find alternative parameters for the stars HD 169730, HD 170174 and HD 170231.

Corrections to the scaling relations from Mosser et al. (2013) were again applied as a test to asteroseismic sample. We observed a typical decrease in the asteroseismic radii of ∼2.5%, which increases the average fractional difference $\langle \Delta R/R_{Ref.} \rangle$ for the asteroseismic targets from -6.58% to -4.31%. and improves the agreement between the two sets of radii. Despite this improvement, we decided to keep our original radii for the same reason as explained for the masses.

As in Section 4.1, we investigated if the offsets between the two sets of radii were correlated with $T_{\rm eff}$, [Fe/H], $V$ magnitude and parallax. No systematic behaviors were found in any case, with maximum correlation coefficients $R^2$ for the weighted linear fits equal to 0.044 for the entire sample (in $T_{\rm eff}$), 0.204 for the binaries (in [Fe/H]) and 0.133 (in parallax) for the asteroseismic targets.

### 4.3. *Surface Gravities*

The last of the three parameters that was derived from both model-independent and -dependent methods is the surface gravity. The comparison between the two sets of results is shown in Figure 5. The agreement is remarkable, with average absolute and percentage differences 0.01 ± 0.01 dex and 0.71 ± 0.51%. Such a good agreement is also observed for the subsamples of binaries and asteroseismic targets. The more robust results for the surface gravity are expected since this parameter (rather than the mass or radius) is directly connected to the asteroseismic observables through the scaling relations (e.g., Kjeldsen & Bedding 1995). Moreover, as noted by Gai et al. (2011), the errors on asteroseismic masses and radii have a strong positive correlation that compensate each other to produce small uncertainties in log g. For this reason, the usage of masses and radii derived from corrected scaling relations (following the prescription from Mosser et al. 2013) to calculate corrected surface gravities leads to virtually equal values of log g.

As was the case for both mass and radius, no systematic trends were observed in the percentage differences between the two sets of surface gravities as a function of any of the input parameters ($T_{\rm eff}$, [Fe/H], $V$ magnitude and parallax). The higher correlation coefficients $R^2$ for the weighted linear fits were 0.039 for the entire sample (in [Fe/H]), 0.041 for the binaries (in [Fe/H]) and 0.107 (in $T_{\rm eff}$) for the asteroseismic targets.

### 4.4. *Ages*

The ages for all our benchmark stars were also given as an output by PARAM (see Table 2), but we were not able to compare them with the literature values because these were also determined using theoretical isochrones. Although not all ages were helpful in assessing the performance of the evolutionary track method, the ones derived for binary systems which have both members in our sample can provide important information about the consistency of our results. The determination of ages for a binary system usually requires that both stars are described by a single isochrone at a given age, which is a reasonable assumption considering the stars were presumably born at the same time from the same molecular cloud. However, we did not impose this constraint here and analyzed members of a given system as if they were individual isolated stars. Thus, a good agreement between the ages derived for the stars in a binary system could be regarded as a consistency check for the results obtained with the evolutionary track method.

Our sample contains 10 systems for which both stars were analyzed: 7 from the LMC, 2 from the SMC and one from the MW. The comparison between the ages of the members is shown in Figure 6. We can see the overall agreement is good, with only three systems not having ages that agree within $1\sigma$: OGLE SMC 130.5 4296, OGLE LMC-ECL-09660 and OGLE LMC-ECL-26122. For OGLE SMC 130.5 4296, the A component has a model-dependent mass 37% higher than the dynamical one, which is consistent with its lower age relative to the B component. A similar situation is observed for OGLE LMC-ECL-09660, with the only difference that it is the B component that has a larger model-dependent mass (by 27%). For the system OGLE LMC-ECL-26122, both

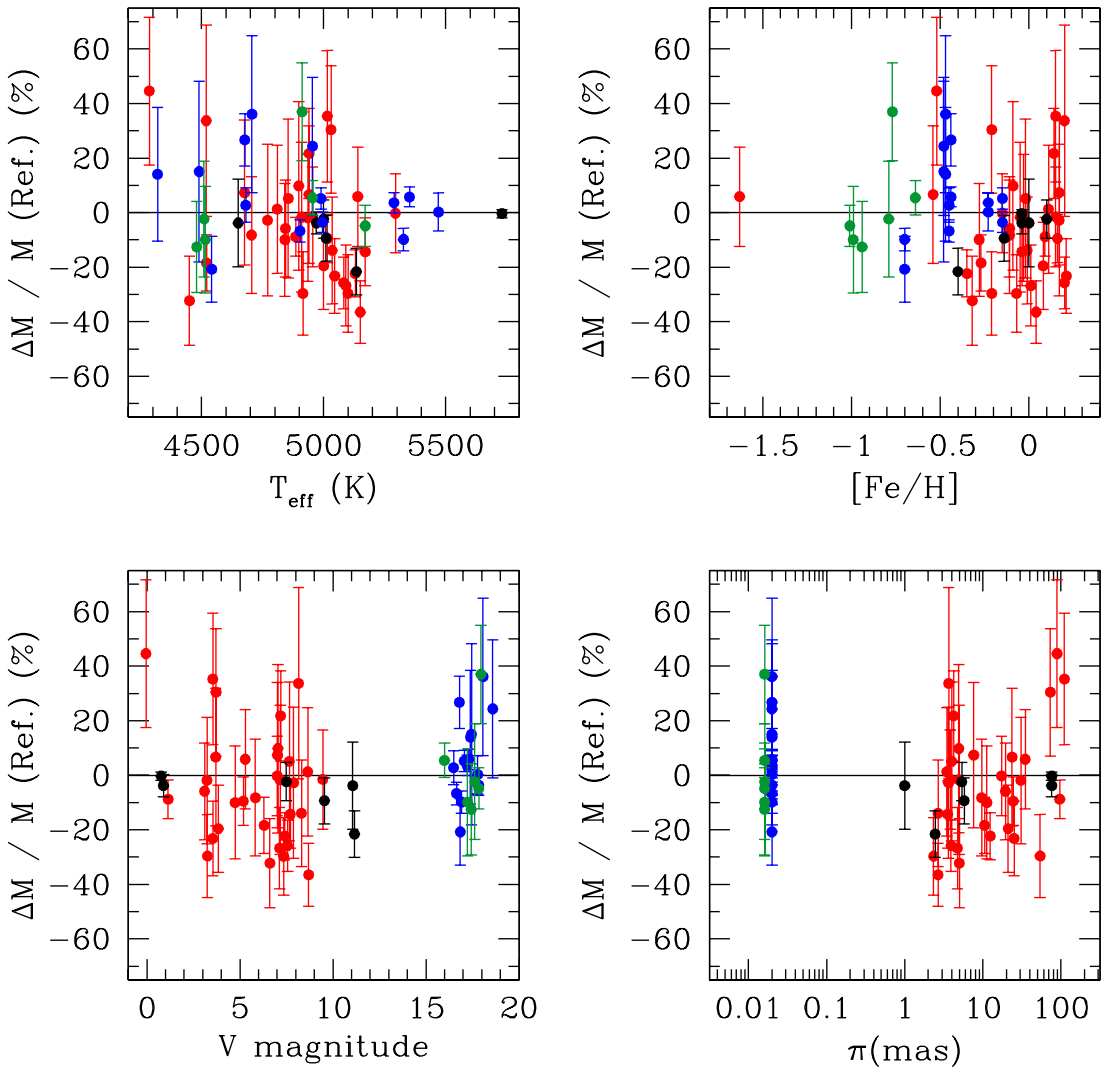


**Figure 3.** Percentage difference between evolutionary track and reference masses as a function of $T_{\rm eff}$ (upper left panel), [Fe/H] (upper right panel), $V$ magnitude (lower left panel) and $\pi$ (lower right panel). Symbols and lines are the same as in Figure 2. We observe no systematic trends for any of the parameters.

components present a good agreement between the two sets of mass (5% for A and -4% for B). However, the small offsets in opposite directions are enough to cause the age discrepancy, especially because of the relatively small errors.

The average absolute and fractional differences between the ages of the components (in the sense A-B) are -0.15 ± 0.13 Gyr and -15.08 ± 13.80 % (where the errors are standard deviations of the mean). A weighted linear fit to the residuals does not show any systematic trends ($R^2 = 0.033$). Thus, the consistency check with the ages provides additional support to the good performance of the evolutionary track method for evolved stars.

## 5. CONCLUSIONS

The determination of masses for evolved stars (subgiants and giants) is still a matter of debate due to recent claims in the literature that the interpolation of observed properties (such as $T_{\rm eff}$, $\log(L/L_{\odot})$ and [Fe/H]) in a grid of evolutionary tracks could yield systematically overestimated results. The accuracy of this method has not been extensively tested in this region of the Hertzsprung–Russell diagram. In order to address this issue, we compiled a sample of 59 benchmark stars from the literature, which includes 26 members of binary systems (in the MW, SMC and LMC) and 33 objects with global asteroseismic parameters.

We determined model-dependent masses for all stars using the PARAM model-grid interpolation code and then compared with model-independent values coming from dynamical (binaries) or asteroseismic (single stars) mass measurements. We observed a very good agreement for the entire mass interval between ∼0.7 – 4.5 $M_{\odot}$, even though a heterogeneous data set was used in the study. The average absolute and fractional differences between model-dependent and reference masses are $-0.10 \pm 0.05$ $M_{\odot}$ and $-1.30 \pm 2.42$%, respectively (where the errors are standard deviations of the means). No sig-

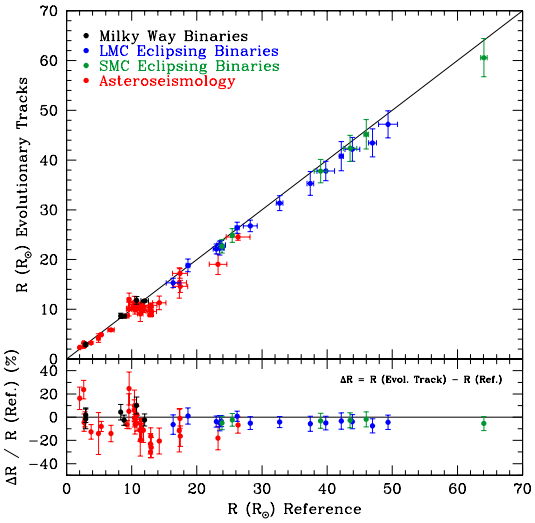


**Figure 4.** Comparison between evolutionary track and reference radii. Symbols, lines and panels are the same as in Figure 2. We can see there is a general good agreement between the radii with small offsets between the two sets of measurements.

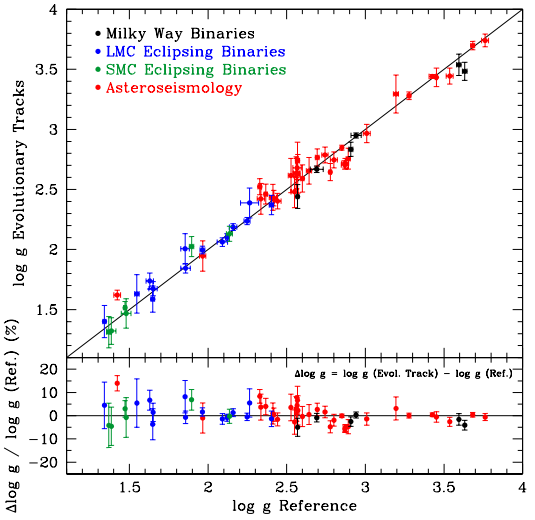


**Figure 5.** Comparison between evolutionary track and reference surface gravities. Symbols, lines and panels are the same as in Figure 2. We can see there is a general good agreement between the gravities and no significant offsets introduced by by the evolutionary track method.

nificant trends in the residuals were found as a function of reference mass, $T_{\rm eff}$, [Fe/H], $V$ magnitude and $\pi$ ($R^2 \leq 0.12$). Similar good agreements were also found for the radii and surface gravities. The analysis of the ages of binary systems provided an additional confirmation that the results obtained with the evolutionary tracks were consistent.

The global results of our study suggest that the interpolation of observed parameters in a grid of evolutionary tracks, in particular the PARSEC set, is capable of providing accurate and relatively precise masses, radii and surface gravities for evolved stars with different effective temperatures and metallicities. We acknowledge, however, that much work remains to be done both observationally and theoretically in order to derive more

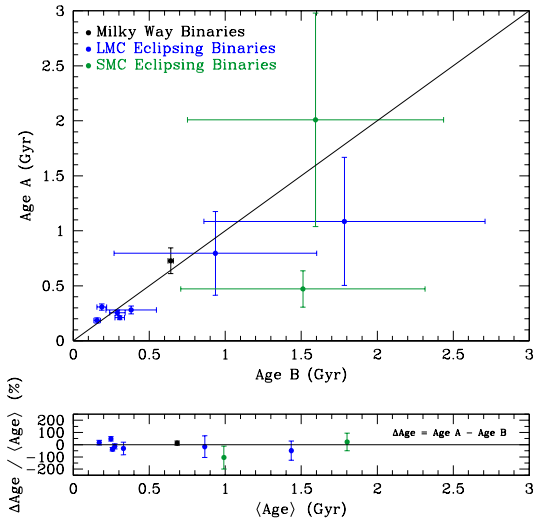


**Figure 6.** Comparison between the ages of the members in binary systems. Symbols and lines are the same as in Figure 2. The upper panel shows a direct comparison of the ages. The lower panel shows the differences (in the sense A-B, relative to the mean age of the system and as a percentage) between the two sets of ages relative to the average age of the system. We can see there is a general good agreement between the ages.

accurate input parameters, improve the models and better understand why some specific stars present a poor agreement in our comparisons.

With this in mind, our team is currently working on a follow-up study that will repeat the analysis done here using different sets evolutionary tracks. This test could potentially determine the physics or free parameters that best reproduce the model-independent masses. We are simultaneously working on the detailed characterization of other potential benchmark stars using interferometry and asteroseismology, in a similar fashion as was done for HD 185351 (Johnson et al. 2014). Finally, in the light of these new results, we plan to revisit the sample of retired A stars from Johnson et al. (2010a), presenting new analyzes of their spectroscopic and kinematic properties.

This research has made use of DEBCat and the SIMBAD database, operated at CDS, Strasbourg, France.

The authors would like to thank Leo Girardi for providing the PARAM code as well as Daniel Huber, Victor Silva Aguirre, Thierry Morel and Nadège Lagarde for kindly sharing their asteroseismic data. We are also grateful to Leo Girardi, Willie Torres, Daniel Huber, Ben Montet, Enrico Corsaro, Saskia Hekker, Scott Fleming, Marc Pinnsoneault, Sarbani Basu and Andrea Miglio for helpful suggestions and discussions.

LG would like to thank the financial support from Coordenação de Aperfeiçoamento de Pessoal de Nível Superior (CAPES), Ciência sem Fronteiras, Harvard College Observatory, and Fundação Lemann. JAJ is grateful for the generous grant support provided by the Alfred P. Sloan and David & Lucile Packard foundations.

## REFERENCES

Adibekyan, V. Z., Santos, N. C., Sousa, S. G., et al. 2012, A&A, 543, AA89

Adibekyan, V. Z., González Hernández, J. I., Delgado Mena, E., et al. 2014, A&A, 564, LL15
Andersen, J. 1991, A&A Rev., 3, 91
Andersen, J., Clausen, J. V., Nordstrom, B., Tomkin, J., & Mayor, M. 1991, A&A, 246, 99
Andersen, J., Clausen, J. V., Nordstrom, B., Gustafsson, B., & Vandenberg, D. A. 1988, A&A, 196, 128
Ando, H., Tsuboi, Y., Kambe, E., & Sato, B. 2010, PASJ, 62, 1117
Baines, E. K., McAlister, H. A., ten Brummelaar, T. A., et al. 2011, ApJ, 743, 130
Bean, J. L., Benedict, G. F., & Endl, M. 2006, ApJ, 653, L65
Beck, P. G., Kambe, E., Hillen, M., et al. 2015, A&A, 573, AA138
Becker, J. C., Johnson, J. A., Vanderburg, A., & Morton, T. D. 2015, arXiv:1503.03874
Berta, Z. K., Irwin, J., & Charbonneau, D. 2013, ApJ, 775, 91
Bonfils, X., Delfosse, X., Udry, S., et al. 2013, A&A, 549, AA109
Bouchy, F., & Carrier, F. 2003, Ap&SS, 284, 21
Bowler, B. P., Johnson, J. A., Marcy, G. W., et al. 2010, ApJ, 709, 396
Bressan, A., Marigo, P., Girardi, L., et al. 2012, MNRAS, 427, 127
Brogaard, K., Sandquist, E., Jessen-Hansen, J., Grundahl, F., & Frandsen, S. 2014, arXiv:1409.2271
Brogaard, K., VandenBerg, D. A., Bruntt, H., et al. 2012, A&A, 543, A106
Bruntt, H., Basu, S., Smalley, B., et al. 2012, MNRAS, 423, 122
Bruntt, H., Bedding, T. R., Quirion, P.-O., et al. 2010, MNRAS, 405, 1907
Buchhave, L. A., Bizzarro, M., Latham, D. W., et al. 2014, Nature, 509, 593
Carrier, F., De Ridder, J., Baudin, F., et al. 2010, A&A, 509, AA73
Canto Martins, B. L., Lèbre, A., Palacios, A., et al. 2011, A&A, 527, AA94
Corsaro, E., Grundahl, F., Leccia, S., et al. 2012, A&A, 537, AA9
Crepp, J. R., & Johnson, J. A. 2011, ApJ, 733, 126
Demarque, P., Woo, J.-H., Kim, Y.-C., & Yi, S. K. 2004, ApJS, 155, 667
Demarque, P., Guenther, D. B., Li, L. H., Mazumdar, A., & Straka, C. W. 2008, Ap&SS, 316, 31
Dotter, A., Chaboyer, B., Jevremović, D., et al. 2008, ApJS, 178, 89
da Silva, L., Girardi, L., Pasquini, L., et al. 2006, A&A, 458, 609
de Medeiros, J. R., Setiawan, J., Hatzes, A. P., et al. 2009, A&A, 504, 617
do Nascimento, J. D., Jr., Charbonnel, C., Lèbre, A., de Laverny, P., & De Medeiros, J. R. 2000, A&A, 357, 931
Döllinger, M. P., Hatzes, A. P., Pasquini, L., et al. 2007, A&A, 472, 649
Döllinger, M. P., Hatzes, A. P., Pasquini, L., et al. 2009, A&A, 499, 935
Epstein, C. R., Elsworth, Y. P., Johnson, J. A., et al. 2014, ApJ, 785, L28
Figueira, P., Faria, J. P., Delgado-Mena, E., et al. 2014, A&A, 570, AA21
Fischer, D. A., & Valenti, J. A. 2005, ApJ, 622, 1102
Frandsen, S., Carrier, F., Aerts, C., et al. 2002, A&A, 394, L5
Frandsen, S., Lehmann, H., Hekker, S., et al. 2013, A&A, 556, AA138
Gai, N., Basu, S., Chaplin, W. J., & Elsworth, Y. 2011, ApJ, 730, 63
Galland, F., Lagrange, A.-M., Udry, S., et al. 2005, A&A, 443, 337
Garcia, E. V., Stassun, K. G., Pavlovski, K., et al. 2014, AJ, 148, 39
Ghezzi, L., Cunha, K., Schuler, S. C., & Smith, V. V. 2010a, ApJ, 725, 721
Ghezzi, L., Cunha, K., Smith, V. V., de Araújo, F. X., Schuler, S., & de la Reza, R. 2010b, ApJ, 720, 1290
Girardi, L., Bertelli, G., Bressan, A., et al. 2002, A&A, 391, 195
Gonzalez, G. 1997, MNRAS, 285, 403
Graczyk, D., Pietrzyński, G., Thompson, I. B., et al. 2014, ApJ, 780, 59
Graczyk, D., Pietrzyński, G., Thompson, I. B., et al. 2012, ApJ, 750, 144
Hatzes, A. P., & Zechmeister, M. 2007, ApJ, 670, L37
Hatzes, A. P., Guenther, E. W., Endl, M., et al. 2005, A&A, 437, 743
Hatzes, A. P., Zechmeister, M., Matthews, J., et al. 2012, A&A, 543, AA98
Hekker, S., Debosscher, J., Huber, D., et al. 2010, ApJ, 713, L187
Hekker, S., & Meléndez, J. 2007, A&A, 475, 1003
Hekker, S., Elsworth, Y., De Ridder, J., et al. 2011, A&A, 525, AA131
Hrivnak, B. J., & Milone, E. F. 1984, ApJ, 282, 748
Huber, D., Bedding, T. R., Stello, D., et al. 2011, ApJ, 743, 143
Huber, D., Carter, J. A., Barbieri, M., et al. 2013, Science, 342, 331
Huber, D., Ireland, M. J., Bedding, T. R., et al. 2012, ApJ, 760, 32
Huber, D., Silva Aguirre, V., Matthews, J. M., et al. 2014, ApJS, 211, 2
Jacobson, H. R., Pilachowski, C. A., & Friel, E. D. 2011, AJ, 142, 59
Jofré, E., Petrucci, R., Saffe, C., et al. 2014, arXiv:1410.6422
Johnson, J. A. 2008, , in ASP Conf. Ser. 398, Extreme Solar Systems, ed. D. Fischer, F. A. Rasio, S. E. Thorsett, & A. Wolszczan (San Francisco, CA:ASP), 59
Johnson, J. A., Aller, K. M., Howard, A. W., & Crepp, J. R. 2010, PASP, 122, 905
Johnson, J. A., Butler, R. P., Marcy, G. W., et al. 2007, ApJ, 670, 833
Johnson, J. A., Clanton, C., Howard, A. W., et al. 2011, ApJS, 197, 26
Johnson, J. A., Fischer, D. A., Marcy, G. W., et al. 2007, ApJ, 665, 78
Johnson, J. A., Howard, A. W., Bowler, B. P., et al. 2010, PASP, 122, 701
Johnson, J. A., Huber, D., Boyajian, T., et al. 2014, ApJ, 794, 15
Johnson, J. A., Marcy, G. W., Fischer, D. A., et al. 2006, ApJ, 652, 1724
Johnson, J. A., Morton, T. D., & Wright, J. T. 2013, ApJ, 763, 53
Jones, M. I., Jenkins, J. S., Bluhm, P., Rojo, P., & Melo, C. H. F. 2014, A&A, 566, AA113
Kallinger, T., Guenther, D. B., Matthews, J. M., et al. 2008, A&A, 478, 497
Kallinger, T., Weiss, W. W., Barban, C., et al. 2010, A&A, 509, A77
Kennedy, G. M., & Kenyon, S. J. 2008, ApJ, 673, 502
Kjeldsen, H., & Bedding, T. R. 1995, A&A, 293, 87
Kjeldsen, H., Bedding, T. R., Arentoft, T., et al. 2008, ApJ, 682, 1370
Lagarde, N., Miglio, A., Eggenberger, P., et al. 2015, arXiv:1505.01529
Lagrange, A.-M., Desort, M., Galland, F., Udry, S., & Mayor, M. 2009, A&A, 495, 335
Laughlin, G., Bodenheimer, P., & Adams, F. C. 2004, ApJ, 612, L73
Lee, B.-C., Mkrtichian, D. E., Han, I., Kim, K.-M., & Park, M.-G. 2011, A&A, 529, A134
Lillo-Box, J., Barrado, D., Moya, A., et al. 2014, A&A, 562, AA109
Lloyd, J. P. 2011, ApJ, 739, L49
Lloyd, J. P. 2013, ApJ, 774, L2
Lovis, C., & Mayor, M. 2007, A&A, 472, 657
Maldonado, J., Villaver, E., & Eiroa, C. 2013, A&A, 554, AA84
Maness, H. L., Marcy, G. W., Ford, E. B., et al. 2007, PASP, 119, 90
Marconi, M., Molinaro, R., Bono, G., et al. 2013, ApJ, 768, LL6
Mayor, M., Lovis, C., & Santos, N. C. 2014, Nature, 513, 328
Miglio, A., Brogaard, K., Stello, D., et al. 2012, MNRAS, 419, 2077
Montgomery, K. A., Marschall, L. A., & Janes, K. A. 1993, AJ, 106, 181
Morel, T., Miglio, A., Lagarde, N., et al. 2014, A&A, 564, AA119
Mortier, A., Santos, N. C., Sousa, S. G., et al. 2013, A&A, 557, AA70
Mosser, B., Goupil, M. J., Belkacem, K., et al. 2012, A&A, 540, AA143
Mosser, B., Michel, E., Belkacem, K., et al. 2013, A&A, 550, AA126
Niedzielski, A., Villaver, E., Wolszczan, A., et al. 2015, A&A, 573, A36
Nielsen, E. L., Liu, M. C., Wahhaj, Z., et al. 2013, ApJ, 776, 4
Omiya, M., Han, I., Izumioura, H., et al. 2012, PASJ, 64, 34

Perryman, M. A. C., Lindegren, L., Kovalevsky, J., et al. 1997, A&A, 323, L49
Pietrzyński, G., Graczyk, D., Gieren, W., et al. 2013, Nature, 495, 76
Pilecki, B., Graczyk, D., Pietrzyński, G., et al. 2013, MNRAS, 436, 953
Pinheiro, F. J. G., Fernandes, J. M., Cunha, M. S., et al. 2014, MNRAS, 445, 2223
Pols, O. R., Tout, C. A., Schroder, K.-P., Eggleton, P. P., & Manners, J. 1997, MNRAS, 289, 869
Quintana, E. V., Barclay, T., Raymond, S. N., et al. 2014, Science, 344, 277
Quirrenbach, A., Amado, P. J., Caballero, J. A., et al. 2014, Proc. SPIE, 9147, 91471F
Ramírez, I., & Allende Prieto, C. 2011, ApJ, 743, 135
Ramírez, I., & Meléndez, J. 2005, ApJ, 626, 465
Ratajczak, M., Hełminiak, K. G., Konacki, M., & Jordán, A. 2013, MNRAS, 433, 2357
Reffert, S., Bergmann, C., Quirrenbach, A., Trifonov, T., Künstler, A. 2015, A&A, 574, AA116
Sabby, J. A., & Lacy, C. H. S. 2003, AJ, 125, 1448
Sandberg Lacy, C. H., Torres, G., & Claret, A. 2012, AJ, 144, 167
Santos, N. C., Israelian, G., & Mayor, M. 2005, A&A, 415, 1153
Sato, B., Izumiura, H., Toyota, E., et al. 2007, ApJ, 661, 527
Sato, B., Kambe, E., Takeda, Y., et al. 2005, PASJ, 57, 97
Schlaufman, K. C., & Winn, J. N. 2013, ApJ, 772, 143
Silva Aguirre, V., Casagrande, L., Basu, S., et al. 2012, ApJ, 757, 99
Sousa, S. G., Santos, N. C., Israelian, G., Mayor, M., & Udry, S. 2011, A&A, 533, 141
Sousa, S. G., Santos, N. C., Mortier, A., et al. 2015, A&A, 576, A94
Southworth, J. 2014, arXiv:1411.1219
Stello, D., Bruntt, H., Preston, H., & Buzasi, D. 2008, ApJ, 674, L53
Takeda, Y., Sato, B., & Murata, D. 2008, PASJ, 60, 781
Takeda, Y., & Tajitsu, A. 2015, arXiv:1503.07595
Tarrant, N. J., Chaplin, W. J., Elsworth, Y., Spreckley, S. A., & Stevens, I. R. 2008, A&A, 483, L43
Teske, J. K., Cunha, K., Smith, V. V., Schuler, S. C., & Griffith, C. A. 2014, ApJ, 788, 39
Thygesen, A. O., Frandsen, S., Bruntt, H., et al. 2012, A&A, 543, AA160
Tian, Z., Bi, S., Bedding, T. R., & Yang, W. 2015, arXiv:1506.01108
Torres, G., Andersen, J., & Giménez, A. 2010, A&A Rev., 18, 67
Torres, G., Claret, A., Pavlovski, K., & Dotter, A. 2015, ApJ, 807, 26
Twarog, B. A., Ashman, K. M., & Anthony-Twarog, B. J. 1997, AJ, 114, 2556
Udalski, A., Szymanski, M. K., Soszynski, I., & Poleski, R. 2008, Acta Astron., 58, 69
Valenti, J. A., & Fischer, D. A. 2005, ApJS, 159, 141
van Leeuwen, F. 2007, A&A, 474, 653
van Leeuwen, F. 2009, A&A, 497, 209
Vandenberg, D. A. 1985, ApJS, 58, 711
Vandenberg, D. A., & Hrivnak, B. J. 1985, ApJ, 291, 270
White, T. R., Bedding, T. R., Stello, D., et al. 2011, ApJ, 743, 161
Zechmeister, M., Reffert, S., Hatzes, A. P., Endl, M., & Quirrenbach, A. 2008, A&A, 491, 531

**Table 1**
Properties of the Benchmark Stars.

| Star | $V$ | $E(B-V)$ | $\pi$ (mas) | $T_{\rm eff}$ (K) | [Fe/H] | $\nu_{\rm max}$ ($\mu$Hz) | $\Delta\nu$ ($\mu$Hz) |
|---|---|---|---|---|---|---|---|
| | | | Binary Stars | | | | |
| AI Phe B | 9.542 ± 0.025 | 0.020 ± 0.020 | 5.78000 ± 0.37000 | 5010 ± 120 | -0.14 ± 0.10 | ··· | ··· |
| CapellaA | 0.892 ± 0.016 | 0.000 | 75.99400 ± 0.08900 | 4970 ± 50 | -0.04 ± 0.06 | ··· | ··· |
| CapellaB | 0.763 ± 0.015 | 0.000 | 75.99400 ± 0.08900 | 5730 ± 60 | -0.04 ± 0.06 | ··· | ··· |
| | | | Stars with Asteroseismology | | | | |
| 11 Com | 4.740 ± 0.020 | 0.016 ± 0.020 | 11.25000 ± 0.22000 | 4841 ± 100 | -0.28 ± 0.10 | 26.70 ± 1.34 | 2.88 ± 0.06 |
| Arcturus | -0.050 ± 0.010 | 0.000 | 88.83000 ± 0.54000 | 4286 ± 30 | -0.52 ± 0.04 | 3.47 ± 0.17 | 0.82 ± 0.02 |
| $\beta$ Aql | 3.710 ± 0.009 | 0.000 | 73.00000 ± 0.20000 | 5030 ± 80 | -0.21 ± 0.07 | 416.00 ± 20.80 | 29.56 ± 0.10 |

**Note**. — A portion of the table is shown here for guidance regarding its form and content. The complete table is available at `https://drive.google.com/file/d/0B_C74xx43AOHTXBKNDh1YVI4RDA/view?usp=sharing`.
AI Phe B: Individual $V$ magnitude was calculated from the value of $M_v$ in Andersen et al. (1988) considering the reddening. $E(B-V)$ from Hrivnak & Milone (1984). Parallax from Torres et al. (2010). $T_{\rm eff}$ and [Fe/H] from Andersen et al. (1988).
Capella A and B: Individual $V$ magnitudes, parallaxes, $T_{\rm eff}$s and [Fe/H] from Torres et al. (2015). $E(B-V) = 0.000$ because d $\lesssim$ 60 pc.
11 Com: $V$ magnitude from SIMBAD. $E(B-V)$ converted from $A_V$ in Takeda et al. (2008) and an arbitrary error of 0.02 was adopted. Parallax from van Leeuwen (2007). $T_{\rm eff}$ and [Fe/H] from Takeda et al. (2008). $\nu_{\rm max}$ and $\Delta\nu$ from Ando et al. (2010). Arbitrary errors of 5% and 2% in $\nu_{\rm max}$ and $\Delta\nu$, respectively.
Arcturus: $V$ magnitude from SIMBAD with an arbitrary error $\sigma(V) = 0.01$. $E(B-V) = 0.000$ because d $\lesssim$ 60 pc. Parallax from van Leeuwen (2007). $T_{\rm eff}$ and [Fe/H] from Ramírez & Allende Prieto (2011). $\nu_{\rm max}$ and $\Delta\nu$ from Lagarde et al. (2015).
$\beta$ Aql: $V$ magnitude from SIMBAD. $E(B-V) = 0.000$ because d $\lesssim$ 60 pc. Parallax from van Leeuwen (2007). $T_{\rm eff}$ and [Fe/H] from Bruntt et al. (2010). $\nu_{\rm max}$ and $\Delta\nu$ from Corsaro et al. (2012). Arbitrary error of 5% in $\nu_{\rm max}$.

**Table 2**
Evolutionary parameters for the benchmark stars.

| Star | Reference Parameters $M$ ($M_\odot$) | $R$ ($R_\odot$) | $\log g$ | PARAM Results $M$ ($M_\odot$) | $R$ ($R_\odot$) | $\log g$ | Age (Gyr) | References |
|---|---|---|---|---|---|---|---|---|
| Binary Stars | | | | | | | | |
| AI Phe B | 1.234 ± 0.004 | 2.932 ± 0.048 | 3.595 ± 0.014 | 1.118 ± 0.104 | 2.889 ± 0.246 | 3.538 ± 0.089 | 6.616 ± 2.122 | Torres et al. (2010) |
| Capella A | 2.569 ± 0.007 | 11.980 ± 0.570 | 2.691 ± 0.041 | 2.472 ± 0.104 | 11.690 ± 0.285 | 2.668 ± 0.027 | 0.727 ± 0.117 | Torres et al. (2015) |
| Capella B | 2.483 ± 0.007 | 8.830 ± 0.330 | 2.941 ± 0.032 | 2.474 ± 0.036 | 8.604 ± 0.212 | 2.950 ± 0.021 | 0.641 ± 0.017 | Torres et al. (2015) |
| Stars with Asteroseismology | | | | | | | | |
| 11 Com | 2.435 ± 0.423 | 17.457 ± 1.141 | 2.335 ± 0.022 | 2.192 ± 0.330 | 14.607 ± 1.212 | 2.422 ± 0.128 | 0.931 ± 0.381 | This work |
| Arcturus | 0.676 ± 0.121 | 26.319 ± 1.829 | 1.422 ± 0.022 | 0.978 ± 0.057 | 24.533 ± 0.663 | 1.621 ± 0.040 | 8.616 ± 1.653 | This work |
| $\beta$ Aql | 0.872 ± 0.133 | 2.624 ± 0.134 | 3.536 ± 0.022 | 1.140 ± 0.105 | 3.248 ± 0.125 | 3.444 ± 0.066 | 5.859 ± 1.868 | This work |

**Note**. — A portion of the table is shown here for guidance regarding its form and content. The complete table is available at `https://drive.google.com/file/d/0B_C74xx43AOHTXBKNDh1YVI4RDA/view?usp=sharing`.

[a] The reference parameters are from the analysis of the RVs and light curves of the eclipsing binary system. The parameters derived from asteroseismology are: M = 1.717 ± 0.142 $M_\odot$, R = 11.480 ± 0.434 $R_\odot$ and log g = 2.552 ± 0.006. The two sets of results agree within 1.6$\sigma$.

**Table 3**
Stars not Included in the Analysis.

| Star | References | Note |
|---|---|---|
| ASAS 010538 B | Ratajczak et al. (2013) | [Fe/H] dependent on stellar evolution models |
| ASAS 182510 A,B | Ratajczak et al. (2013) | [Fe/H] dependent on stellar evolution models |
| ASAS 182525 A,B | Ratajczak et al. (2013) | [Fe/H] depends on stellar evolution models |
| $\beta$ Oph | Kallinger et al. (2010) | Error on reference mass >20% |
| $\beta$ UMi | Tarrant et al. (2008) | Error on reference mass >20% |
| CF Tau A | Sandberg Lacy et al. (2012) | [Fe/H] dependent on stellar evolution models |
| $\epsilon$ Tau | Ando et al. (2010) | Suspicious (too high) reference mass |
| $\eta$ Her | Ando et al. (2010) | Suspicious (too high) reference mass |
| HD 50890 | Lagarde et al. (2015) | Error on reference mass >20% |
| HD 169751 | Lagarde et al. (2015) | Error on reference mass >20% |
| HD 170031 | Lagarde et al. (2015) | No independent parallax available |
| HD 170053 | Lagarde et al. (2015) | Error on reference mass >20% |
| HD 175679 | Lagarde et al. (2015) | Error on reference mass >20% |
| $\iota$ Dra | Zechmeister et al. (2008); Baines et al. (2011) | No value for $\Delta\nu$ |
| Kepler-56 | Huber et al. (2013) | No independent parallax available |
| Kepler-91 | Lillo-Box et al. (2014) | No independent parallax available |
| KIC 3730953 | Takeda & Tajitsu (2015) | Parallax error too large |
| KIC 5737655 | Huber et al. (2012) | Error on reference mass >20% |
| KIC 6442183 | Tian et al. (2015) | No independent parallax available |
| KIC 9705687 | Thygesen et al. (2012) | Parallax error too large |
| KIC 11137075 | Tian et al. (2015) | No independent parallax available |
| KIC 11674677 | Huber et al. (2011) | Error on reference mass >20% |
| M67 13 | Kallinger et al. (2010) | Distance is not model-independent |
| OGLE SMC113.3 4007 A | Graczyk et al. (2012) | Assumed [Fe/H] |
| OGLE LMC CEP0227 B | Pilecki et al. (2013); Marconi et al. (2013) | [Fe/H] depends on pulsation models |
| OGLE LMC-ECL-10567 A,B | Pietrzyński et al. (2013) | Remarks about the results for the system |

**Note**. — There are 11 K giants in Stello et al. (2008), but the values of $\Delta\nu$ are not provided.

**Table 4**
Statistics for the comparison between evolutionary track and reference parameters.

| Sample | $N_{Stars}$ | $\langle \Delta Par \rangle$[a] | $\langle \Delta Par / Par_{Ref.} \rangle$[a] (%) | A[b] | B[b] | $R^2$ | $\sigma$ |
|---|---|---|---|---|---|---|---|
| | | | Par = M ($M_\odot$) | | | | |
| All Stars | 59 | $-0.095 \pm 0.052$ | $-1.30 \pm 2.42$ | $0.60 \pm 1.65$ | $-3.76 \pm 4.79$ | 0.002 | 1.32 |
| Binaries | 26 | $0.041 \pm 0.065$ | $2.49 \pm 2.99$ | $0.57 \pm 1.93$ | $-2.24 \pm 5.76$ | 0.004 | 1.34 |
| Asteroseismology | 33 | $-0.202 \pm 0.073$ | $-4.29 \pm 3.58$ | $-11.53 \pm 2.93$ | $12.12 \pm 6.75$ | 0.333 | 0.89 |
| | | | Par = R ($R_\odot$) | | | | |
| All Stars | 59 | $-1.002 \pm 0.172$ | $-4.81 \pm 1.32$ | $0.00 \pm 0.07$ | $-5.07 \pm 1.86$ | 0.000 | 1.26 |
| Binaries | 26 | $-1.033 \pm 0.214$ | $-2.57 \pm 0.73$ | $-0.11 \pm 0.04$ | $0.45 \pm 1.21$ | 0.268 | 0.49 |
| Asteroseismology | 33 | $-0.978 \pm 0.261$ | $-6.58 \pm 2.25$ | $-0.74 \pm 0.36$ | $-0.54 \pm 4.10$ | 0.122 | 1.44 |
| | | | Par = log g | | | | |
| All Stars | 59 | $0.010 \pm 0.011$ | $0.71 \pm 0.51$ | $-1.14 \pm 0.60$ | $3.04 \pm 1.77$ | 0.061 | 1.22 |
| Binaries | 26 | $0.003 \pm 0.015$ | $0.49 \pm 0.74$ | $-2.05 \pm 0.68$ | $4.74 \pm 1.70$ | 0.277 | 0.75 |
| Asteroseismology | 33 | $0.015 \pm 0.016$ | $0.89 \pm 0.70$ | $-1.28 \pm 1.14$ | $3.70 \pm 3.56$ | 0.040 | 1.48 |

[a] $\Delta Par = Par_{Trk.}$ - $Par_{Ref.}$, where Par can be mass, radius or surface gravity. The uncertainties are standard deviations of the means.
[b] Coefficients of the linear fit $y = Ax + B$.